

A Relativistic-Plasma Compton Maser

James C. Weatherall

*Department of Physics
New Mexico Institute of Mining and Technology
Socorro NM 87801*

ABSTRACT

A relativistic pair-plasma which contains a high excitation of electrostatic turbulence could produce intense radiation at brightness temperature in excess of 10^{20} K by stimulated scattering. Important relativistic effects include the broadband frequency response of the plasma, and Compton-boosting of the scattered radiation. In radio-frequency relativistic plasma, the optical depth can be as small as tens of meters. When the plasma wave excitation is one-dimensional and particle distributions have $T_{\perp} \ll T_{\parallel}$, the frequency-dependent angular distribution of the emission exhibits characteristics of pulsar emission.

Subject headings: instabilities — plasmas — pulsars: general — radiation mechanisms: non-thermal

1. Introduction

Radio emission at extremely high brightness temperature is possible by stimulated scattering in astrophysical plasmas with a high degree of plasma turbulence. Intensities on the order of 10^{20} to 10^{30} K are suspected in some astrophysical objects, and an emission process of the form of a plasma maser may explain the extraordinary intensity at radio frequencies of pulsars (Melrose 1996) and active galactic nuclei (Wagner & Witzel 1996). The following calculation exhibits the intensity and spectrum of emission in a relativistic plasma of electrons and positrons under the assumption of a uniform and high degree of excitation of plasma electrostatic wavemodes. It shows that the path length through the plasma can be relatively small for radiative growth; that Compton-like scattering increases the mean emission frequency above the plasma frequency; and the frequency bandwidth of the emission is fairly narrow despite the broadband excitation in the plasma.

The calculation is done in a relativistic regime because pair plasmas derive from extremely energetic processes such as gamma-ray annihilation. Simulations of pair plasma creation (Arendt & Eilek 2001) show that the pair-plasma distribution functions can be described by a thermal parameter which is moderately relativistic. In this paper, the kinetic temperature parameter $\rho = mc^2/(k_B T_K)$ is assigned a value of 1/10.

Conversion into electromagnetic modes by scattering on plasma waves in nonrelativistic space plasma is known to produce radiation at the plasma frequency $\omega_p = (4\pi ne^2/m_e)^{1/2}$, and wave-wave coalescence at twice the plasma frequency (Gurnett et al. 1981). Radiation at these well-defined frequencies is due to the narrow frequency response in the plasma. It seems obvious that emission in a relativistic plasma is unlikely to follow this plasma emission paradigm. For one thing, electrostatic modes in a relativistic plasma exist over a broad range of frequencies, $\omega_p\sqrt{\rho} < \omega < \omega_p/\sqrt{\rho}$ (Godfrey et al. 1975a,b; Melrose et al. 2000). Furthermore, scattering by relativistic particles can modify frequencies by factors of $4\gamma^2$. Still, the stimulated emission appears to be fairly narrow in frequency, but this is a characteristic of maser emission due to frequency-dependent growth acting over many growth lengths.

Although this solution is illustrative of relativistic effects in plasma emission, several assumptions are used to simplify calculation. First, the excitation of the turbulence is characterized by a single temperature parameter without regard to specific plasma-streaming or shock-excitation mechanisms, or wave cascades. For example, in thermal equilibrium the energy density in plasma waves relative to kinetic energy density, $E^2/(8\pi nk_B T_K)$, is inversely proportional to the number of particles in a Debye cube, $n\lambda_D^3 = n[c/(\omega_p\sqrt{\rho})]^3$. This parameter can be quite large for astrophysical plasmas. If a radio-frequency plasma ($\nu_p \sim 3GHz$) manages an equipartition between turbulent electrostatic energy and thermal kinetic energy at temperatures of $T_K \sim 5 \times 10^{10} K$, the characteristic excitation as described by an enhanced temperature $T_{NL} = (n\lambda_D^3)T_K$ could be more than $10^{22} K$. This coherent enhancement of scattering on plasma waves was recognized by Gailaitis et al. (1964), and Colgate et al. (1970).

Another simplification is to do the calculation without an imposed background magnetic field. This justifies the assumption of isotropy in the particle distributions, wave spectra, and wave dispersion. Including a magnetic field would tend to make the turbulence one-dimensional in the direction of the magnetic field, and would modify the dispersion properties of the electromagnetic modes. Thus the plasma maser in a magnetized plasma would not be isotropic in direction, but would have preferred directions for emission. The effect of making the maser plasma one-dimensional is illustrated by an example.

Finally, the turbulent excitation is assumed to be steady. This energy reservoir in turbulence must be maintained by an injection process against the radiation loss, but to model this requires an additional kinetic model for the turbulence. The assumption of constant wave excitation can be expected to fail when the brightness temperature greatly exceeds the wave temperature, and radiation becomes a significant energy sink. Radiative losses will also determine the lifetime of the system.

The calculation proceeds from classical scattering rates between plasma and electromagnetic wave modes. The kinetic equation is put into the form of a radiative transfer equation in the next section, assuming a kinetic temperature for the plasma and a nonlinear effective temperature for the plasma turbulence. The necessary integrals for the scattering coefficients are done numerically

as described in section 3. The intense emission which can derive from the maser process is discussed in section 4.

2. Transfer Equation

We start with a transfer equation between the plasma waves and electromagnetic radiation (see, for example, Melrose (1980), section 5.4). For this equation, the electromagnetic wave spectra is described by the photon number density function, $N^T(\mathbf{k})$, and the plasma wave spectra is described by the number density function $N^L(\mathbf{k})$. (The number density spectrum is also called the occupation number.)

By definition, the number of photons with wavevector \mathbf{k} in a phase space volume d^3k around \mathbf{k} is given by $N(\mathbf{k}) [d^3k/(2\pi)^3]$. The integral of $N(\mathbf{k})$ over phase space will give the number of photons per cm^3 .

The plasmon occupation number can be formulated from the electric field energy spectrum of the turbulent waves,

$$W = \frac{1}{VT} \int \frac{E(\mathbf{r}, t)E(\mathbf{r}, t)}{4\pi} dV dt = \frac{1}{VT} \int \frac{d^3k}{(2\pi)^3} \frac{d\omega}{2\pi} \frac{E^*(\mathbf{k}, \omega)E(\mathbf{k}, \omega)}{4\pi} \quad (1)$$

averaged over time T and volume V . Assuming well-defined wavemodes, $E(\mathbf{k}, \omega) = E(\mathbf{k})2\pi\delta[\omega - \omega^L(\mathbf{k})]$, the integration over ω gives the following:

$$W = \int \left[\frac{1}{V} \frac{E^*(\mathbf{k})E(\mathbf{k})}{4\pi} \right] \left[\frac{d^3k}{(2\pi)^3} \right] \quad . \quad (2)$$

Because the term in second brackets is the number density of wavemodes between \mathbf{k} and $\mathbf{k} + d\mathbf{k}$, it is easy to identify the first term in brackets as the electrostatic energy per wavemode. We apply a thermal-like excitation of normal modes in the turbulence to derive:

$$\frac{1}{V} \frac{E^*(\mathbf{k})E(\mathbf{k})}{4\pi} = \frac{1}{2} k_B T_{NL} \quad . \quad (3)$$

For electrostatic waves, another degree of freedom is invested in the particle motion. Finally, the occupation number is acquired from a semi-classical formula

$$N^L(\mathbf{k}) = \begin{cases} \frac{k_B T_{NL}}{\hbar \omega^L(k)}, & \sqrt{\rho} \omega_p < kc < \omega_p / \sqrt{\rho} \quad ; \\ 0, & \text{otherwise.} \end{cases} \quad (4)$$

The inequality describes the frequency range of plasma normal modes in a relativistic plasma.

With this notation, the transfer equation, in the classical limit, for photons in plasma turbulence is given by (Melrose (1980), eq. 5.89):

$$\begin{aligned} \frac{dN^T(\mathbf{k})}{dt} &= \int \frac{d^3k'}{(2\pi)^3} d^3p n \varpi^{TL}(\mathbf{p}, \mathbf{k}, \mathbf{k}') \\ &\times \left[f(\mathbf{p}) \{N^L(\mathbf{k}') - N^T(\mathbf{k})\} + N^L(\mathbf{k}') N^T(\mathbf{k}) \hbar(\mathbf{k} - \mathbf{k}') \cdot \frac{\partial f}{\partial \mathbf{p}} \right]. \end{aligned} \quad (5)$$

The three-dimensional thermal distribution of lepton momentum in a relativistic plasma is given by the normalized function $f(\mathbf{p})d^3p = \exp(-\rho\gamma(p))/Z d^3p$; here, $Z = (4\pi K_2(\rho))/\rho$, K_2 is the modified Bessel function, $\gamma = [1+p^2/(m^2c^2)]^{1/2}$, and ρ is the temperature parameter. The spatially-averaged number density of particles in the zero-momentum reference frame is n . To write this equation in terms of the specific intensity $I(\omega)$ for a single polarization, use

$$I(\omega)d\omega d\Omega = \hbar\omega N^T(\omega/c)c \frac{k^2 dk d\Omega}{(2\pi)^3} \quad . \quad (6)$$

The resulting equation has three terms. The first term represents spontaneous scattering:

$$\frac{dI}{ds} = \Lambda_1(\omega) \frac{\omega^2}{(2\pi)^3 c^3} k_B T_{NL} \quad , \quad (7)$$

where the emission coefficient has been put into the form

$$\Lambda_1(\omega) = \int \frac{d^3k'}{(2\pi)^3} n f(\mathbf{p}) d^3p \varpi^{TL}(\mathbf{p}, \mathbf{k}, \mathbf{k}') \frac{\omega}{\omega'} \quad . \quad (8)$$

The second term represents absorption

$$c \frac{dI}{ds} = -\Lambda_2(\omega) I(\omega) \quad , \quad (9)$$

where the absorption coefficient is

$$\Lambda_2(\omega) = \int \frac{d^3k'}{(2\pi)^3} n f(\mathbf{p}) d^3p \varpi^{TL}(\mathbf{p}, \mathbf{k}, \mathbf{k}') \quad . \quad (10)$$

The final term contributes to stimulated scattering. For a thermal distribution, the momentum derivative gives

$$\frac{\partial f}{\partial \mathbf{p}} = -\frac{c f(\mathbf{p})}{k_B T} \beta \quad . \quad (11)$$

The vector arithmetic can be worked out using the kinematic relationship between frequencies,

$$\omega' = \omega \frac{1 - \beta \cos \theta}{1 - \beta \cos \theta'} \quad , \quad (12)$$

where the angles are between the wavevectors and the electron velocity vector. Thus,

$$\hbar(\mathbf{k} - \mathbf{k}') \cdot \frac{\partial f}{\partial \mathbf{p}} = -\frac{\hbar\omega}{k_B T} \left[1 - \frac{\omega'}{\omega} \right] f(\mathbf{p}) \quad . \quad (13)$$

The stimulated scattering term is

$$c \frac{dI}{ds} = \frac{T_{NL}}{T} [\Lambda_2(\omega) - \Lambda_1(\omega)] I(\omega) \quad . \quad (14)$$

The complete transfer equation is

$$\frac{dI(\omega)}{ds} = \Lambda_1 \frac{\omega^2 k_B T_{NL}}{(2\pi)^3 c^3} + \left[-\Lambda_2 + \frac{T_{NL}}{T} (\Lambda_2 - \Lambda_1) \right] \frac{I(\omega)}{c} \quad . \quad (15)$$

3. Formulation of the Scattering Coefficients

The probability for scattering of longitudinal waves into transverse waves by relativistic electrons is given by (Melrose (1980), eq 4.150; also Melrose (1971))

$$n\varpi^{TL}(\mathbf{p}, \mathbf{k}, \mathbf{k}') \frac{d^3k'}{(2\pi)^3} = \frac{(2\pi)^3 ne^4}{m^2 \omega' \omega} \frac{(1 - \beta^2)}{(1 - \hat{k} \cdot \beta)^2 (1 - \hat{k}' \cdot \beta)^2} \delta\left(\omega(1 - \hat{k} \cdot \beta) - \omega'(1 - \hat{k}' \cdot \beta)\right) \\ \times \left[(1 - \hat{k} \cdot \beta)^2 (1 - (\hat{k}' \cdot \beta)^2) - (1 - \beta^2)(\hat{k} \cdot \hat{k}' - \hat{k}' \cdot \beta)^2 \right] \frac{d^3k'}{(2\pi)^3} \quad , \quad (16)$$

where use is made of $\omega' = k'c$. $n \varpi^{TL}(\mathbf{p}, \mathbf{k}, \mathbf{k}') d^3k'$ has units s^{-1} . In Equation (16), a sum is made over polarization in the scattered waves.

The integration of the scattering rates over d^3k' and d^3p are done in spherical coordinates in which angle θ' measures \mathbf{k}' relative to β and θ measures β relative to \mathbf{k} . In terms of angle cosines $\mu = \cos \theta$:

$$d^3k' = \frac{\omega'^2}{c^3} d\omega' d\phi' d\mu' \quad ; \\ d^3p = p^2 dp d\phi d\mu \quad . \quad (17)$$

The integral over $d\omega'$ can be done easily with the delta-function. After integration over $d\phi'$ and $d\phi$, the remaining integrals over angle in the emission rate are

$$\Lambda_1(\omega) = \frac{3}{16} n\sigma_{TC} \int 4\pi p^2 f(p) dp \int_{\mu_{min}}^1 \frac{1 - \beta^2}{1 - \beta\mu} d\mu \int_{-1}^{\mu'_{max}} \frac{A + B\mu'^2}{(1 - \beta\mu')^4} d\mu' \quad , \quad (18)$$

where A and B are algebraic functions of μ :

$$A = 1 + \beta^2 - 4\beta\mu + \mu^2 + \beta^2\mu^2 \quad , \\ B = 1 - 5\beta^2 + 2\beta^4 + 4\beta\mu - 3\mu^2 + 3\beta^2\mu^2 - 2\beta^4\mu^2 \quad . \quad (19)$$

The upper cutoff to the $d\mu'$ integral is a byproduct of the delta-function, and the high-frequency bound on $\omega' < (1 + \beta)\gamma\omega_p$. Thus,

$$\mu'_{max} = \min \left\{ \frac{1}{\beta} - \frac{\omega(1 - \beta\mu)}{2\beta\gamma\omega_p}, 1 \right\} \quad (20)$$

In order for μ'_{max} to be larger than -1 , the angles μ must be larger than

$$\mu_{min} = \max \left\{ \frac{1}{\beta} - \frac{1 + \beta}{\beta} \frac{2\gamma\omega_p}{\omega}, -1 \right\} \quad (21)$$

Similarly, the absorption rate

$$\Lambda_2(\omega) = \frac{3}{16} n\sigma_{TC} \int 4\pi p^2 f(p) dp \int_{\mu_{min}}^1 \frac{1 - \beta^2}{(1 - \beta\mu)^2} d\mu \int_{-1}^{\mu'_{max}} \frac{A + B\mu'^2}{(1 - \beta\mu')^3} d\mu' \quad . \quad (22)$$

The integrals in the above equation are completed numerically. Solutions for $\Lambda_1(\omega)$ and $\Lambda_2(\omega)$ are shown in Figure 1. The two scattering rates are equal ($\Lambda_1 \sim \Lambda_2$) near the characteristic frequency $\omega_p(1/\rho^{3/2})$.

4. Amplification by Stimulated Emission

With fixed values for the wave temperature, T_{NL} , and the kinetic temperature, T_K , the transfer equation is a first order differential equation with constant coefficients which can be solved directly as a function of path length:

$$I = I_K e^{s\Lambda_{stim}/c} + I_{NL} \frac{\Lambda_1}{\Lambda_{stim}} \left(e^{s\Lambda_{stim}/c} - 1 \right) \quad , \quad (23)$$

where the effective stimulated scattering rate is

$$\Lambda_{stim}(\omega) = (\Lambda_2 - \Lambda_1) T_{NL}/T_K - \Lambda_2 \quad . \quad (24)$$

At low frequency ($\omega \ll \omega_p \rho^{3/2}$), $\Lambda_1 \gg \Lambda_2$ and the intensity is limited to the kinetic temperature. Near the characteristic frequency, the intensity saturates at the nonlinear wave temperature. At higher frequencies, the intensity increases exponentially. However, the exponentiation rate diminishes at frequencies much higher than the characteristic frequency because Λ_1 and Λ_2 become small.

The high brightness temperatures derived from this theory must be qualified by the fact that cooling of the plasma and the turbulence are not taken into account. A full picture of the energy balance requires additional kinetic equations for the plasma waves and particle energy distribution. However, it is easy to estimate how long the plasma can maintain its relativistic energy against the Compton loss. At $10^{22} K$, a $10^3 cm$ scale system (such as a pulsar magnetospheric source region) will last $10^{-6} s$, and a $10^{14} cm$ scale system (encompassing an AGN accretion region) will last for $10^5 s$ against radiative loss. These simple numbers suggest how maser lifetime might relate to microstructure in pulsar radio emission and intraday variability in QSO's.

To show the magnitude of stimulated emission, the scattering coefficients can be scaled as follows:

$$\frac{s\Lambda}{c} \frac{T_{NL}}{T_K} = 1.3 \times 10^{-10} \frac{T_{NL}}{T_K} \left(\frac{\Lambda}{n\sigma_T c} \right) \left(\frac{n}{10^{11} cm^{-3}} \right) \left(\frac{s}{1000 cm} \right) \quad . \quad (25)$$

Substantial growth in intensity occurs in path lengths smaller than a kilometer assuming turbulence temperatures $T_{NL}/T_K \geq 10^{12}$, as demonstrated in Figure 2. Such a large temperature for the turbulence is not implausible from an energy standpoint. The turbulent temperature estimated from equipartition between electrostatic and plasma kinetic energy is

$$\frac{T_{NL}}{T_K} \sim \left(\frac{c\sqrt[3]{n}}{\omega_p\sqrt{\rho}} \right)^3 = 6 \times 10^{13} \left(\frac{10^{11} cm^{-3}}{n} \right)^{1/2} \left(\frac{0.1}{\rho} \right)^{3/2} \quad . \quad (26)$$

For a plasma kinetic temperature on the order of $10^{10} K$, radiative brightness temperatures greater than $10^{23} K$ are consistent with stimulated emission from this mechanism. Higher brightness temperatures are possible with greater turbulent temperature or larger path lengths, depending on what limits are imposed by Compton cooling.

In summary, the relativistic-plasma Compton maser uses free energy in the form of wave turbulence to produce electromagnetic radiation via induced scattering in the relativistic thermal plasma. The high brightness temperature derives from the large value of the plasma parameter, $n[c/(\omega_p\sqrt{\rho})]^3$ – generally true in astrophysical plasmas, although less so in laboratory plasmas. The maser turbulence conversion mechanism is an alternative to other plasma turbulence conversion processes invoking coherent spatial effects or nonlinear waves dynamics (for example, Weatherall (1997, 1998); Asseo et al. (1990)), which may not develop due to the turbulence being strongly driven or highly inhomogeneous.

The turbulent conversion process described here might also apply to pulsars. Maser models are not new to pulsar radiation physics (for example, Lyutikov et al. (1999); Luo & Melrose (1995)), but these masers resemble free-electron masers in which particle beams generate the emission. A model invoking the Compton plasma-maser requires further inclusion of anisotropies due to the magnetic field, wave dispersion properties in magnetized plasma, and specific mechanisms for wave excitation by collimated particle beams. However, we can simulate these effects by limiting the plasma momentum distribution and turbulent wavevectors to a single coordinate axis.

In one-dimension, the differential scattering cross-sections in terms of the angle cosine μ between the emission wavevector \mathbf{k} and the z -coordinate axis are given by

$$\begin{aligned} \frac{d\Lambda_2(k, \mu)}{d\Omega} &= \int \frac{dk'}{(2\pi)^3} \frac{\omega'^2}{c^2} \int ndpf(p) \omega^{TL}(p, k', \mathbf{k}) \\ \frac{d\Lambda_1(k, \mu)}{d\Omega} &= \int \frac{dk'}{(2\pi)^3} \frac{\omega'^2}{c^2} \int ndpf(p) \left[\frac{1 \pm \beta}{1 - \beta\mu} \right] \omega^{TL}(p, k', \mathbf{k}) \end{aligned} \quad (27)$$

The choice of sign is (+) for electrostatic waves with k' in the *negative* z -direction, and (–) for waves in the *positive* z -direction. The calculation assumes waves have relativistic dispersion relation $\omega' = k'c$, and the uniform excitation applies to frequencies $\omega_p\sqrt{\rho} < \omega' < \omega_p/\sqrt{\rho}$. The one-dimensional electron distribution function is given by $f(p) dp = \exp[-\rho\gamma(p)] dp / (2K_1(\rho))$, where K_1 is the modified Bessel function.

The transfer equation is the same as before, substituting for the scattering rates $\Lambda_1 \rightarrow \Delta\Omega(d\Lambda_1/d\Omega)$ and $\Lambda_2 \rightarrow \Delta\Omega(d\Lambda_2/d\Omega)$. Here, $\Delta\Omega$ is the range of solid angles about the turbulence axis which have the nonlinear excitation. The important difference in one-dimension is the directivity of the maser. Figure 3 is a polar plot in angle and frequency. The emissivity in the plasma rest frame is largest in directions *near* perpendicular to the magnetic axis, with some angular structure due to relativistic thermal velocities. However, the plasma is moving relative to the lab/star frame because of the polar cap current flow, and the emission can be expected to be beamed relativistically: this is illustrated in the figure with a Lorentz transformation.

One intriguing consequence of the moving maser is the angular dependence of the peak emission for different frequencies. Radio pulsars show a variation in pulse profile (intensity vs. phase) for different observing frequency. This is generally interpreted as radius-to-frequency mapping based on the presumption that the emission comes from different heights in the polar cap, and that

the emission frequency is tied to the local plasma frequency. As clearly shown in Figure 4, the maser emission from a single location can produce similar frequency-dependent profiles. Note that the spectrum of the emission is found here to have a fairly steep index in the case of uniform one-dimensional turbulence, $I_\nu \sim \nu^{-3}$.

Finally, we remark that relativistic temperatures have the effect of supporting wave frequencies which are in a broad range about the plasma frequency: still, the highest growth occurs at frequencies above the plasma frequency. Thus, relativistic effects do not appear to mitigate the puzzle that emission at the local plasma frequency in the pulsar polar cap plasma produces frequencies which seem high for radio emission (Melrose & Gedalin 2000; Kunzl et al. 1998).

This work is supported by NSF grants AST-9618408 and AST-9720263. Justin Jayne contributed to evaluating the numerical integrations. Discussions with Paul Arendt, Jean Eilek, and Tim Hankins are gratefully acknowledged.

REFERENCES

- Arendt, P., & Eilek, J. 2001, submitted ApJ
- Asseo, E., Pelletier, G., & Sol, H. 1990, MNRAS 247, 529
- Colgate, S. A., Lee, E. P., & Rosenbluth, M. N. 1970, ApJ 162, 649
- Gailaitis, A., & Tsytovich, V. N. 1964, Sov. Phys. JETP 19, 1164
- Godfrey, B.B., Newberger, B.S., & Taggart, K. 1975, IEEE Trans. on Plasma Sci. PS-3, 60
- Godfrey, B.B., Newberger, B.S., & Taggart, K. 1975, IEEE Trans. on Plasma Sci. PS-3, 68
- Gurnett, D. A., Maggs, J. E., Gallagher, D. L., Kurth, W. S., & Scarf, F. L. 1981, J. Geophys. Res., 86, 8833
- Kunzl, T., Lesch, H., Jessner, A., & von Hoensbroech, A. 1998, ApJ 505, L139
- Luo, Q., & Melrose, D. B. 1995, MNRAS 276, 372
- Lyutikov, M., Machabili, G. Z., & Blandford, R. D. 1999, ApJ 512, 804
- Melrose, D. B. 1971, Astrophys & Sp. Sci. 10, 197.
- Melrose, D. B. 1980, Plasma Astrophysics, vol I (NY: Gordon and Breach)
- Melrose, D. B. 1996 in IAU Colloq. 160, Pulsars: Problems and Progress, ed. S. Johnston, M.A. Walker, & M. Bailes (San Francisco: ASP), 139
- Melrose, D. B., & Gedalin, M. E. 2000, ApJ, in press
- Melrose, D. B., Gedalin, M. E., Kennett, M. .P., and Fletcher, C. S. 2000, J. Plasma Phys., in press
- Wagner, S. J., & Witzel, A. 1996, ARA&A 36, 475
- Weatherall, J. C. 1997, ApJ 483, 402
- Weatherall, J. C. 1998, ApJ 506, 341

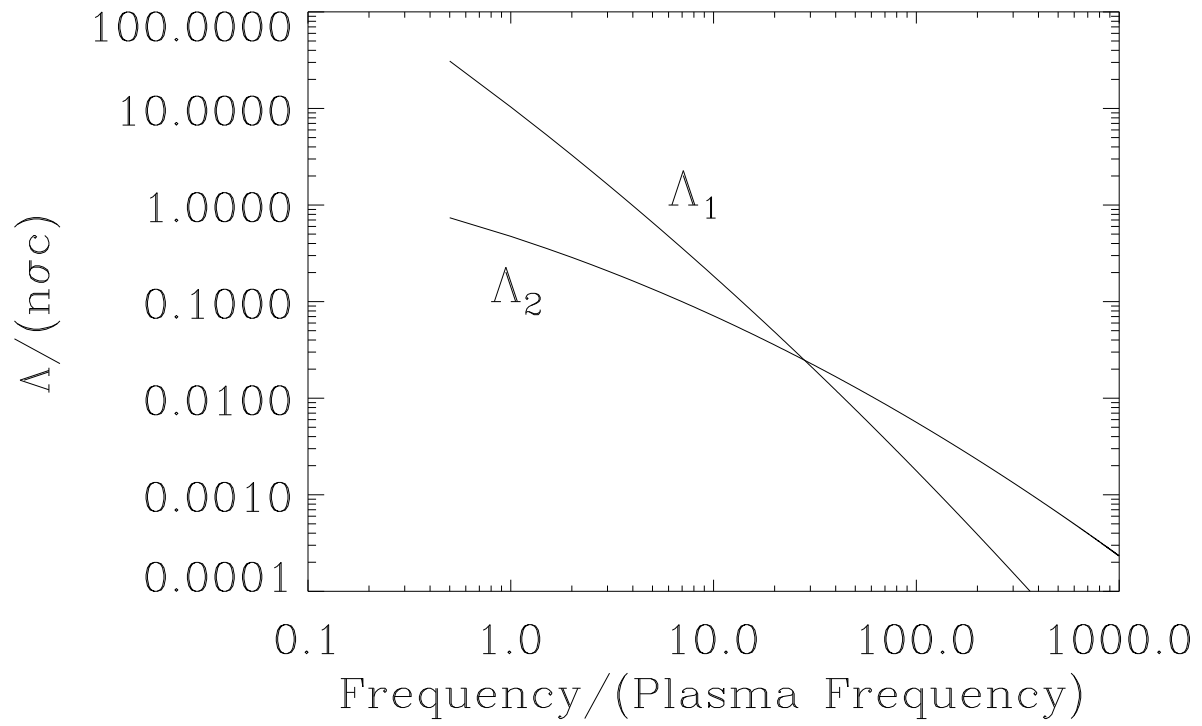


Fig. 1.— Scattering coefficients determined numerically from Eqs. 18 and 22 for isotropic thermal particles of temperature $k_B T_K = 10mc^2$.

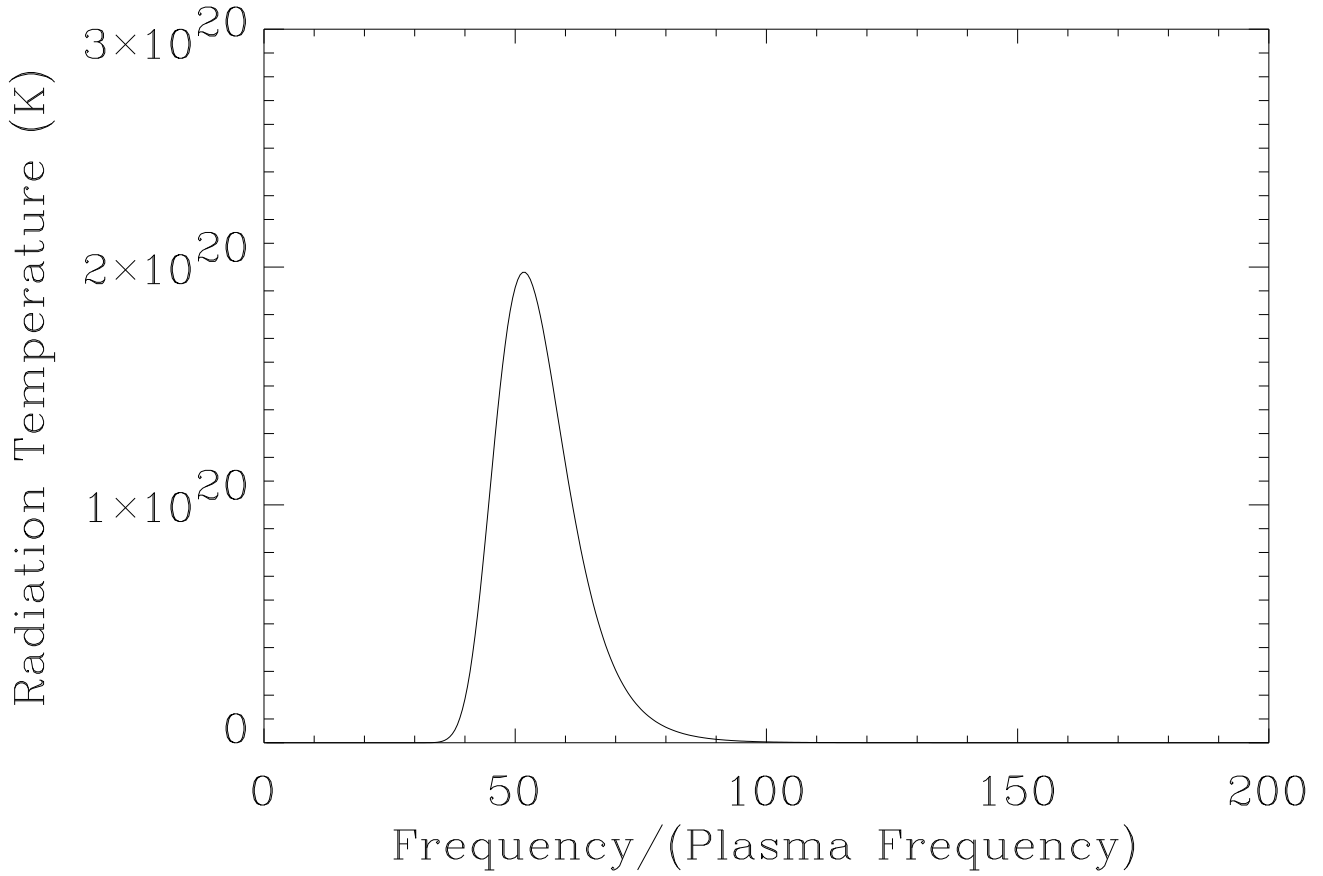


Fig. 2.— Intensity of plasma maser emission in a electron-positron plasma with kinetic temperature of $10mc^2$. The turbulent excitation is taken to be enhanced by $T_{NL}/T_K = 10^{12}$. Scaling to a plasma frequency of $f_0 = 3GHz$, the path length corresponds to $s = 2 \times 10^5$ cm.

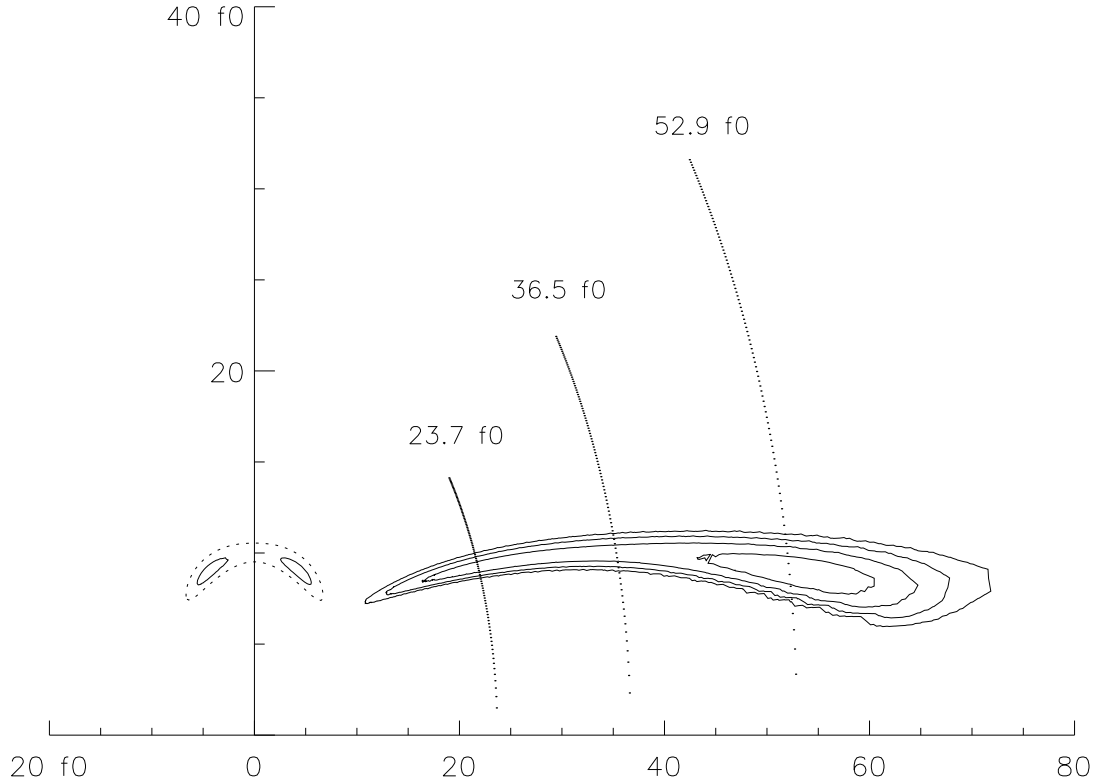


Fig. 3.— Contours of constant brightness temperature in frequency space for the Compton-maser for one-dimensional turbulence with $T_{NL}/T_K = 10^{12}$, and a path length of $s = 1.5 \times 10^6$ cm. The frequency is in units of the plasma frequency, f_0 . The contour levels are $1, 2, 4,$ and 8×10^{16} K. The contours for both the plasma rest frame, and the lab frame in which the plasma moves with $\gamma = 3.8$ are shown: the lowest contour is dotted in the former case. Intensity along the three cuts of constant frequency are presented in the next figure.

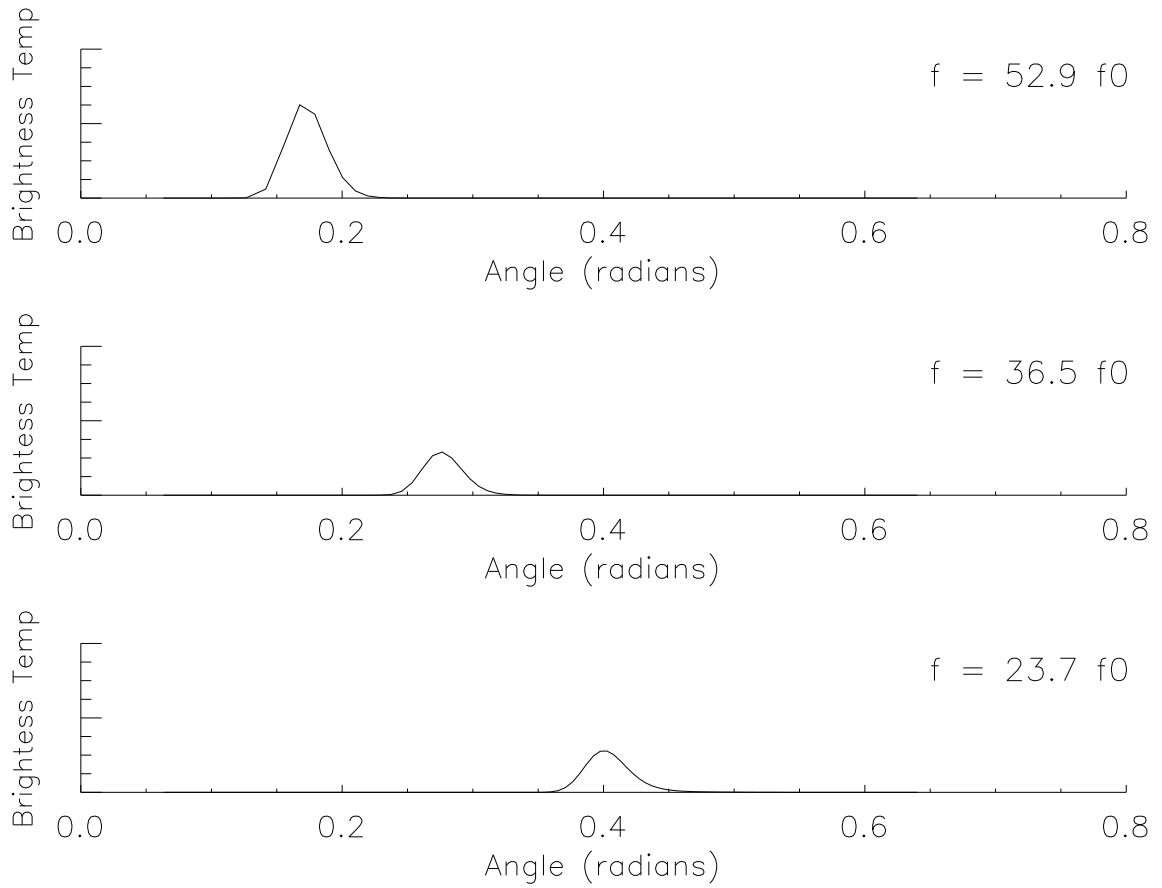


Fig. 4.— Brightness temperature vs. angle for three different frequencies for the case of a moving plasma. The temperature scale is the same for each plot, with a scale maximum at $1.5 \times 10^{17} K$.